Early stages of relativistic fireball expansion

G.S. Bisnovatyi-Kogan
Space Research Institute, 84/32 Profsoyuznaya, 117810 Moscow, Russia

Marina V.A. Murzina
Institute of Theoretical and Experimental Physics, B. Cheremushkinskaya 25, 117259 Moscow, Russia
(Received 20 March 1995)

The expansion of a relativistic fireball is investigated analytically in the frame of relativistic hydrodynamics with an ultrarelativistic equation of state $\varepsilon = 3P$. Equations of spherical flow with Lorentz factors $\gamma \gg 1$ are reduced to a simple form, and we present their general solution. We also get a particular solution, describing a thin spherical shell moving with ultrarelativistic speed—the leading part of a relativistic fireball. A self-similar solution for the central part of the fireball is matched with the outer shell solution, thus giving the general picture of expansion, which is in good agreement with numerical results. The obtained solutions are related to early stages of fireball expansion, appearing in γ-ray bursts of cosmological origin and within multiple production of particles.

PACS number(s): 47.75.+f, 03.30.+p, 13.65.+i, 95.30.Lz

I. INTRODUCTION

The rapid release of a large amount of energy in a small volume leads to the formation of a relativistic fireball, where the temperature exceeds the rest-mass energy of particles [1,2]. Such a release is expected in the cosmological model of γ-ray bursts (GRB's), where an energy $\sim 10^{51}$ ergs is produced in a small volume comparable to the volume of a neutron star with a radius $\sim 10^6$ cm [3,4]. The energy concentration in such a fireball is so high ($\sim 10^{11}$ g/cm^3) that in initial stages of expansion it is always opaque and can be treated in the frame of relativistic hydrodynamics [5,6] as an adiabatic expansion into the vacuum. In the simplest case, the outflow is spherically symmetric.

There are self-consistent analytical solutions for relativistic expansion into the vacuum, but only for plane geometry. Namely, an approximate solution for the plane ultrarelativistic case was derived in [7] and applied to the initial outflow after multiple particle production. An exact solution for the plane-parallel relativistic expansion into the vacuum was obtained in [8]. Reference [9] treated analytically the spherical problem of black hole evaporation, where the matter expands initially "slowly" and forms a sort of atmosphere, decelerating the following motion. Thus no consistent analytical solution for spherical expansion into the vacuum has been constructed so far. In this work, we present an attempt of that kind.

A qualitative analytical and detailed numerical investigation of the fireball expansion as applied to the GRB events has been done in numerous works [10–12,1,2]. The results of numerical modeling show that after a short rearrangement phase, a spherically symmetric relativistic fireball acquires a rather universal structure. Most mass and energy are concentrated in a thin shell which moves ultrarelativistically: nearly at the speed of light c. The central density and temperature decrease with time much faster than those in the leading shell.

Collecting expanding matter into a shell is a purely relativistic effect and occurs because there exists a maximal speed of motion c. This effect could be quantitatively explained as follows. As long as the released energy is much smaller than the rest mass of the object, $E_0 \ll M_0$ (we use units with $c = 1$), expansion is nonrelativistic and typically close to the self-similar regime [13]. At any moment of time, density and pressure have domed radial profiles (maximum at the center), while velocity linearly grows from the center to the edge and is higher as the value of E_0 gets larger. If we now formally apply this nonrelativistic solution to the case $E_0 \gg M_0$, we shall obtain that most layers (except for the very central ones) have velocities $v > c$ even in the earliest stages of expansion. This means that in reality all these layers will move together with $v \simeq c$, i.e., expand in the form of a shell.

Some processes leading to the appearance of the fireballs, such as multiple production of hadrons by electron-positron annihilation[1] [14,15], contain stochastic elements, producing an uncertainty in the initial structure of the fireball. In these cases, initial profiles of hydrodynamic functions can be chosen only very schematically. The best justification for any choice, however, is that the following motion appears to be rather insensitive to the initial profiles. As we mentioned above, numerical cal-

[1]The hadron outflow after e^--e^+ annihilation would be spherically symmetric, because both original particles disappear, and information about initial anisotropy in their motion is lost. Of course, the applicability of the hydrodynamic approach to such outflow is strongly restricted and is related to huge initial energies. However, in a number of works (see [14,15] and references therein), hydrodynamics is employed to describe the earliest stages of hadron motion in this case.

culations with different initial conditions have brought out that, as $t \gg R_0$ (where R_0 is the initial radius), the fireball looks rather universal: an ultrarelativistic shell and rarefaction at the center. We can expect, therefore, that this structure is mainly determined not by the initial conditions but by general properties of expansion; these properties could be mathematically associated with the basic structure of relativistic fluid equations.

In this work, we construct an analytic solution for adiabatic relativistic spherical expansion into the vacuum. This solution consists of two parts. First, we derive equations (linear first-order partial differential equations with constant coefficients) of relativistic spherical flow with Lorentz factors $\gamma \gg 1$. A general solution of these equations is presented in analytical form. We formulate boundary conditions which allow us to get a particular solution, describing an ultrarelativistically moving shell—the main part of the relativistic fireball. Second, we construct a self-similar solution of relativistic fluid equations with arbitrary γ and apply it to the expansion of the matter between the center and the shell. Matching of these two solutions gives the general picture of expansion, which agrees with the results of numerical calculations [1,2]. Note that the outflow cannot be described by a self-similar treatment alone, since the total energy within each similarity solution diverges (see Sec. IV and [15]), which actually means that the value of the initial radius is important for the fireball structure.

In what follows, we consider spherical adiabatic flow with an ultrarelativistic equation of state $\varepsilon = 3P$ (ε is the energy density in the comoving frame, and P is the pressure). Equations of conservation of momentum and energy fluxes read [16]

$$\frac{\partial}{\partial t}(4v\gamma^2\varepsilon) + \frac{\partial}{\partial r}[(4v^2\gamma^2+1)\varepsilon] + \frac{8v^2\gamma^2\varepsilon}{r} = 0\,, \qquad (1.1)$$

$$\frac{\partial}{\partial t}[(4\gamma^2-1)\,\varepsilon] + \frac{\partial}{\partial r}\left(4v\gamma^2\varepsilon\right) + \frac{8v\gamma^2\varepsilon}{r} = 0\,. \qquad (1.2)$$

Here, v is the hydrodynamic velocity, $\gamma=(1-v^2)^{-1/2}$ is the Lorentz factor, and we use units with $c=1$. Multiplying (1.1) by v and subtracting (1.2) we arrive at an entropy ($s = \text{const} \times \varepsilon^{3/4}$) conservation equation

$$\frac{\partial}{\partial t}\left(\gamma\,\varepsilon^{3/4}\right) + \frac{\partial}{\partial r}\left(v\,\gamma\,\varepsilon^{3/4}\right) + \frac{2}{r}\,\gamma\,v\,\varepsilon^{3/4} = 0\,. \qquad (1.3)$$

We can write separately the equation of the baryon charge conservation:

$$\frac{\partial}{\partial t}\left(\gamma\,N_b\right) + \frac{\partial}{\partial r}\left(v\,\gamma\,N_b\right) + \frac{2}{r}\,\gamma\,v\,N_b = 0\,, \qquad (1.4)$$

where N_b is the baryon charge density (excess of baryons over antibaryons) in the comoving frame.

II. EQUATIONS OF ULTRARELATIVISTIC SPHERICAL FLOW

In this section, we derive hydrodynamic equations for ultrarelativistic motion: $v \simeq 1$, $\gamma \gg 1$. In the next section, we apply these equations to the main part of the expanding flow — the leading shell.

For any ultrarelativistically moving layer, its distance $\xi = t-r$ from the light surface ($r = t$) approaches a constant [7]: $d\xi/dt = 1-v \approx 1/(2\gamma^2) \ll 1$. This makes ξ a suitable variable related to a Lagrangian coordinate. Introduce the variables ($\xi = t-r$, r) instead of (t, r) in Eqs. (1.1), (1.2). After subtracting these equations from each other and leaving the second one and the difference of them, we obtain

$$\begin{aligned}
&\frac{\partial}{\partial\xi}\left\{\left[4\gamma^2(1-v)-1\right]\varepsilon\right\} + \frac{\partial}{\partial r}\left(4v\gamma^2\varepsilon\right) + \frac{8v\gamma^2\varepsilon}{r} = 0\,,\\
&\frac{\partial}{\partial\xi}\left[4\gamma^2(1-v)^2\varepsilon\right] + \frac{\partial}{\partial r}\left\{\left[4v\gamma^2(1-v)-1\right]\varepsilon\right\} \qquad (2.1)\\
&\qquad + \frac{8}{r}\,v\,(1-v)\,\gamma\,\varepsilon = 0\,.
\end{aligned}$$

For the case of plane geometry, there exists an exact analytical solution [8], describing expansion into the vacuum with arbitrary γ. In the spherical case, the last terms in (2.1) break this opportunity. So we use the approximation $\gamma \gg 1$ similar to [7] with $v \simeq 1$, $(1-v) \simeq 1/(2\gamma^2)$, which gives

$$\begin{aligned}
&\frac{\partial\varepsilon}{\partial\xi} + \frac{\partial}{\partial r}\left(4\gamma^2\varepsilon\right) + \frac{8}{r}\,\gamma^2\varepsilon = 0\,,\\
&\frac{\partial}{\partial\xi}\left(\frac{\varepsilon}{\gamma^2}\right) + \frac{\partial\varepsilon}{\partial r} + \frac{4\varepsilon}{r} = 0\,.
\end{aligned} \qquad (2.2)$$

Similar approximate equations for the plane-parallel case, treated in [7], do not contain the last terms of (2.2) (without derivatives), which are of the main order in the spherical case. We use here another procedure for finding an analytical solution.

For spherical motion with $\gamma \to \infty$, the momentum and energy equations (1.1), (1.2) are reduced to a divergent form, leading to the relation $\gamma^2\,\varepsilon = \text{const}/r^2$. On the other hand, at late stages of expansion with small pressure, any element of matter expands uniformly in the comoving frame, so that its thickness grows as $h_{\text{com}} \propto r$, while in the laboratory frame, the thickness h_{lab} of the layer remains constant. Recalling that $h_{\text{com}} = \gamma h_{\text{lab}}$, we get the basic relations of ultrarelativistic spherical flow (see also [7,1,2]):

$$\gamma \propto r\,, \qquad \varepsilon \propto r^{-4} \qquad (2.3)$$

(in the plane case, $\gamma \propto \sqrt{r}$). To describe the particular structure of the flow, we introduce the new functions

$$g = \gamma^2/r^2\,, \qquad \varepsilon_1 = \varepsilon\, r^4, \qquad (2.4)$$

and a new variable $y = 1/r$ (instead of r). Substitution of (2.4) into Eqs. (2.2) reduces the main terms of the type of (2.3) and yields

$$\begin{aligned}
&\frac{\partial\varepsilon_1}{\partial\xi} - 4\,\frac{\partial(\varepsilon_1\,g)}{\partial y} = 0\,,\\
&\frac{\partial}{\partial\xi}\left(\frac{\varepsilon_1}{g}\right) - \frac{\partial\varepsilon_1}{\partial y} = 0\,.
\end{aligned} \qquad (2.5)$$

Transferring in (2.5) to the variable τ instead of ε_1,

$$\varepsilon_1 = \varepsilon_{10}\,e^{-4\tau}\,, \quad \varepsilon_{10} \text{ is an arbitrary constant,} \qquad (2.6)$$

we obtain,

$$\frac{\partial\tau}{\partial\xi} - 4g\frac{\partial\tau}{\partial y} + \frac{\partial g}{\partial y} = 0\,,$$
$$\frac{\partial g}{\partial\xi} + 12g^2\frac{\partial\tau}{\partial y} - 4g\frac{\partial g}{\partial y} = 0\,. \tag{2.7}$$

Assuming that the Jacobian $\Delta = \partial(\tau, g)/\partial(\xi, y)$ is not equal to zero in the case of interest, we make the Legendre transformation of Eqs. (2.7), i.e., replace the functions and variables. As a result, we get equations for $\xi(\tau, g)$ and $y(\tau, g)$:

$$\frac{\partial y}{\partial g} + 4g\frac{\partial\xi}{\partial g} + \frac{\partial\xi}{\partial\tau} = 0\,,$$
$$\frac{\partial y}{\partial\tau} + 12g^2\frac{\partial\xi}{\partial g} + 4g\frac{\partial\xi}{\partial\tau} = 0\,. \tag{2.8}$$

Using the variable φ instead of g,

$$g = g_0\, e^{2\varphi}\,, \quad g_0 \text{ is an arbitrary constant,} \tag{2.9}$$

and introducing the function

$$y_1 = \frac{y}{2g} = \frac{y}{2g_0\, e^{2\varphi}} = \frac{r}{2\gamma^2} \tag{2.10}$$

instead of y, we come to a set of linear partial differential equations with constant coefficients:

$$2\frac{\partial\xi}{\partial\varphi} + \frac{\partial\xi}{\partial\tau} + \frac{\partial y_1}{\partial\varphi} + 2y_1 = 0\,,$$
$$3\frac{\partial\xi}{\partial\varphi} + 2\frac{\partial\xi}{\partial\tau} + \frac{\partial y_1}{\partial\tau} = 0\,. \tag{2.11}$$

This is a hyperbolic set of equations with the eigenvalues $\mp 1/\sqrt{3}$ and the characteristics

$$x_1 = \tau - \frac{\varphi}{\sqrt{3}} = \text{const}\,,$$
$$x_2 = \tau + \frac{\varphi}{\sqrt{3}} = \text{const}\,. \tag{2.12}$$

Using the pair of characteristical variables $\{x_1, x_2\}$ instead of $\{\varphi, \tau\}$, we rewrite the set (2.11) in the most compact form:

$$\frac{\partial}{\partial x_1}\left[\left(1-\frac{2}{\sqrt{3}}\right)\xi - \frac{1}{\sqrt{3}}y_1\right] = -y_1\,,$$
$$\frac{\partial}{\partial x_2}\left[\left(1+\frac{2}{\sqrt{3}}\right)\xi + \frac{1}{\sqrt{3}}y_1\right] = -y_1\,. \tag{2.13}$$

Equations (2.13) [or (2.11)] with the variables defined in (2.4), (2.6), (2.9), (2.10), and (2.12) describe relativistic adiabatic spherical flow with the relativistic factor $\gamma \gg 1$.

A general solution of (2.11) can be obtained as follows. Increasing the derivative order we get a separate equation of the second order for ξ:

$$3\left(\frac{\partial^2\xi}{\partial\varphi^2} + 2\frac{\partial\xi}{\partial\varphi}\right) - \left(\frac{\partial^2\xi}{\partial\tau^2} - 4\frac{\partial\xi}{\partial\tau}\right) = 0 \tag{2.14}$$

and exactly the same equation for y_1. Both equations are solved using the standard procedure of variable separation. Substituting their solutions into (2.11), we get relations between the constants of integration and obtain a general solution in the form

$$\xi = -\int \alpha\varepsilon_1^{-\alpha/4}\left\{\chi_1(\alpha)\, g^{\beta_1/2} + \chi_2(\alpha)\, g^{\beta_2/2}\right\}d\alpha,$$
$$y_1 = \int \varepsilon_1^{-\alpha/4}\left\{(3\beta_1+2\alpha)\chi_1(\alpha)\, g^{\beta_1/2} + (3\beta_2+2\alpha)\,\chi_2(\alpha)\, g^{\beta_2/2}\right\}d\alpha. \tag{2.15}$$

Here, $\beta_1(\alpha)$ and $\beta_2(\alpha)$ are the roots of the square equation $3(\beta^2+2\beta)+(-\alpha^2+4\alpha) = 0$, while $\chi_1(\alpha)$, $\chi_2(\alpha)$ are arbitrary functions determined by the initial and boundary conditions. In the physical variables $\{t, r, \varepsilon, \gamma\}$, the general solution can be written as

$$t-r = \int \frac{-\alpha}{r^\alpha\varepsilon^{\alpha/4}}\left\{\chi_1(\alpha)\left(\frac{\gamma}{r}\right)^{\beta_1} + \chi_2(\alpha)\left(\frac{\gamma}{r}\right)^{\beta_2}\right\}d\alpha\,,$$
$$\frac{r}{\gamma^2} = \int \frac{2}{r^\alpha\,\varepsilon^{\alpha/4}}\left\{(3\beta_1+2\alpha)\,\chi_1(\alpha)\left(\frac{\gamma}{r}\right)^{\beta_1} + (3\beta_2+2\alpha)\,\chi_2(\alpha)\left(\frac{\gamma}{r}\right)^{\beta_2}\right\}d\alpha\,. \tag{2.16}$$

For getting a particular solution, we use the set (2.13) with characteristic variables x_1, x_2. After differentiating (2.13), we obtain separate equations of second order for $\xi(x_1, x_2)$ and for $y_1(x_1, x_2)$. Each of these equations can be tranformed to the classical telegraphic equation

$$\frac{\partial^2 f(x_1,x_2)}{\partial x_1\,\partial x_2} - \frac{1}{4}f(x_1,x_2) = 0 \tag{2.17}$$

and the same equation for the function $\tilde{f}(x_1, x_2)$, where

$$f = e^{-(1+\sqrt{3}/2)\,x_1}e^{-(1-\sqrt{3}/2)\,x_2}\xi(x_1,x_2)\,,$$
$$\tilde{f} = e^{-(1+\sqrt{3}/2)\,x_1}e^{-(1-\sqrt{3}/2)\,x_2}y_1(x_1,x_2)\,. \tag{2.18}$$

The Riemann-Green function of Eq. (2.17) is [17]

$$R(x_1,x_2;\,x_1',x_2') = I_0\left(\sqrt{(x_1-x_1')\,(x_2-x_2')}\right), \tag{2.19}$$

where I_0 is the Bessel function of an imaginary argument. The relations along the characteristics $x_2 = \text{const}$ and $x_1 = \text{const}$ can be obtained by changing partial derivatives in (2.13) to full derivatives and returning to the variables (φ, y) from (2.10) and (2.12). These relations can be also reduced to

$$dy = -4g_0\left(1-\sqrt{3}/2\right)e^{2\varphi}\,d\xi \qquad (x_2 = \text{const})\,, \tag{2.20}$$

$$dy = -4g_0\left(1+\sqrt{3}/2\right)e^{2\varphi}\,d\xi \qquad (x_1 = \text{const})\,. \tag{2.21}$$

III. ULTRARELATIVISTIC SHELL

The outer part of relativistic fireball (the shell) contains most of the matter and moves ultrarelativistically.

We apply the equations of the previous section to describe the structure of the shell and must formulate the initial and the boundary conditions.

Assume that both the leading and the trailing edges of the shell can be treated as free boundaries, i.e., the edges with the vacuum. For the leading edge, the assumption is valid as long as the ambient density and pressure can be neglected. As for the inner boundary, we actually assume that the central part of the flow (inner with respect to the shell) contains comparatively small energy and entropy, and this flow cannot essentially effect the motion of the shell. This assumption agrees with the following results of our treatment and with numerical results [1,2] as well.

Free boundaries correspond to the characteristics of fluid equations. We solve here a boundary problem in the variables x_1, x_2, avoiding initial conditions in the (t, r) plane, which means that we choose boundary functions on two time-dependent spherical surfaces. Note that we thus consider an evolved expansion at $t \gg R_0$ with the structure of the fireball, shaped by the expansion process itself. So really the boundaries should be mathematically produced by the basic structure of the outflow equations, i.e., to coincide with the characteristics.

We specify boundary conditions along $x_1 = \text{const} = 0$ and $x_2 = \text{const} = 0$ and solve Eq. (2.18). Here, the constants are taken equal to zero; as a whole, we can choose them arbitrarily by redefining the free coefficients ε_{10} and g_0 in (2.6), (2.9). For $f(x_1, x_2)$, the problem can be formulated as

$$\begin{aligned} \frac{\partial^2 f}{\partial x_1\, \partial x_2} - \frac{1}{4} f &= 0 , \\ f\big|_{x_1=0} &= f_1(x_2) , \\ f\big|_{x_2=0} &= f_2(x_1) , \end{aligned} \tag{3.1}$$

where the functions f_1 and f_2 present the boundary conditions: $f_1(0) = f_2(0)$. This is a characteristic Cauchy problem [17,18], which can be solved by a standard tecnique of Riemann-Green function (2.19), giving

$$\begin{aligned} f(x_1, x_2) = f_1(0) I_0(\sqrt{x_1 x_2}) &+ \int_0^{x_2} \frac{d f_1(x_2')}{dx_2'} I_0\big(\sqrt{x_1 (x_2 - x_2')}\big)\, dx_2' \\ &+ \int_0^{x_1} \frac{d f_2(x_1')}{dx_1'} I_0\big(\sqrt{(x_1 - x_1') x_2}\big)\, dx_1' . \end{aligned} \tag{3.2}$$

The same solution is valid for the function $\tilde{f}$ with boundary functions $\tilde{f}_1(x_2)$ and $\tilde{f}_2(x_1)$. Let us specify the boundary functions f_1, f_2, $\tilde{f}_1$, and $\tilde{f}_2$.

The leading edge of the shell is associated with the boundary $x_1 = 0$, i.e., $\tau = \varphi/\sqrt{3}$, while the inner edge is represented by the boundary $x_2 = 0$, i.e., $\tau = -\varphi/\sqrt{3}$. Formation of the cavity inside the shell and vacuum outside implies a condition of decreasing energy density ε to zero on both boundaries. We get then, from (2.4), (2.6),

$$\tau = -\frac{1}{4} \ln \frac{\varepsilon_1}{\varepsilon_{10}} = -\frac{1}{4} \ln \frac{\varepsilon r^4}{\varepsilon_{10}} \gg 1 \qquad \text{at } x_1 \to 0 \quad \text{or} \quad x_2 \to 0 . \tag{3.3}$$

At the outer boundary we have

$$\varphi = \sqrt{3}\tau \gg 1 , \qquad x_2 = \tau + \frac{\varphi}{\sqrt{3}} = 2\tau \gg 1 \tag{3.4}$$

and, at the inner boundary,

$$\varphi = -\sqrt{3}\tau \gg 1 , \qquad x_1 = \tau - \frac{\varphi}{\sqrt{3}} = 2\tau \gg 1 . \tag{3.5}$$

From relations (2.6), (2.9) we get the connections on the outer boundary,

$$\begin{aligned} &e^{x_1} = e^{\tau - \varphi/\sqrt{3}} = 1 , \qquad e^{x_2} = e^{\tau + \varphi/\sqrt{3}} = e^{2\tau} , \\ &g = g_0 e^{\sqrt{3} x_2} , \qquad \varepsilon_1 = \varepsilon_{10} e^{-2x_2} \qquad \text{at } x_1 = 0 \end{aligned} \tag{3.6}$$

and, on the inner boundary:

$$\begin{aligned} &e^{x_2} = e^{\tau + \varphi/\sqrt{3}} = 1 , \qquad e^{x_1} = e^{\tau - \varphi/\sqrt{3}} = e^{2\tau} , \\ &g = g_0\, e^{-\sqrt{3} x_1} , \qquad \varepsilon_1 = \varepsilon_{10}\, e^{-2x_1} \qquad \text{at } x_2 = 0 . \end{aligned} \tag{3.7}$$

Let us suggest that the matter at the outer edge approaches the speed of light c, and so we choose, for this boundary,

$$\xi = \xi^{(1)} = \xi_{a1} + \xi_a\, e^{-k x_2} , \qquad x_1 = 0 , \tag{3.8}$$

where ξ_{a1}, ξ_a, and k are constant parameters defined below. Solving (2.21), we have, for the outer boundary,

$$y_1 = y_1^{(1)} = \xi_a\, y_a\, e^{-k x_2} , \qquad y_a = k\, \frac{\sqrt{3} + 2}{\sqrt{3} - k} . \tag{3.9}$$

In order to have decreasing y (increasing r) on the outer edge, $y \sim g\, y_1 \sim e^{(\sqrt{3} - k) x_2}$, we must choose $k > \sqrt{3}$, what implies $\xi_a < 0$, $y_a < 0$ (y_1 must be positive). This means, according to (3.8), that the difference $(t - r)$ for this edge increases with time, tending to the constant value ξ_{a1}, when v rapidly approaches c.

As for the trailing edge, we assume that expansion of the innermost layers of the shell approaches a self-similar character. In the next section, we construct this self-similar solution in detail. Here it is enough to note that the (r, t) dependence is reduced to the dependence on one variable

$$\eta = \frac{r}{t} = \left(1 + \frac{\xi}{r}\right)^{-1} \tag{3.10}$$

in any self-similar relativistic problem, since there exists a dimensional parameter of the speed of light. The inner boundary can be characterized by the fixed value of η_{fit}:

$$\xi y = \delta_{\text{fit}} = \frac{1}{\eta_{\text{fit}}} - 1 . \tag{3.11}$$

This implies $dy = -(\delta_{\text{fit}}/\xi^2)\, d\xi$ to be substituted into Eq. (2.20) and thus yields

$$\xi = \xi^{(2)} = \xi_b\, e^{\sqrt{3} x_1/2} , \qquad \xi_b = \left[\frac{\delta_{\text{fit}}}{2 g_0 (2 - \sqrt{3})}\right]^{1/2} . \tag{3.12}$$

Formally, there is also a trivial solution $\xi = \text{const}$, but it corresponds to $y = 1/r = \text{const}$ and is not the case of interest when we consider expansion. Definition (2.10), together with (3.11) and (3.12), gives

$$y_1 = y_1^{(2)} = \frac{\delta_{\text{fit}}}{2g_0}\,\frac{e^{\sqrt{3}\,x_1}}{\xi^{(2)}} = (2-\sqrt{3})\,\xi_b\,e^{\sqrt{3}\,x_1/2}. \quad (3.13)$$

Having in mind that the self-similar regime and, hence, relation (3.11) should be approached asymptotically at sufficiently great times $t \gg R_0$ (where R_0 is the initial radius of the fireball), which corresponds to $\xi^{(2)} \gg 1$ as $x_1 \gg 1$ [see (3.5)], we can treat (3.12) as the main-order term of the solution and take $\xi^{(2)}$ in the form

$$\xi^{(2)} = \xi_b e^{\sqrt{3}\,x_1/2} + \xi_{b1}\ . \quad (3.14)$$

Here, ξ_{b1} is an arbitrary constant, negligible when compared to the first term (as $x_1 \gg 1$). As we argue below, boundary relation (3.14) with $\xi_{b1} \neq 0$ could be more sensible physically.

As a result, using (2.19), (3.8), (3.9), (3.13), (3.14) we get the following relations for the boundary functions:

$$\begin{aligned} f_1(x_2) &= \left(\xi_{a1} + \xi_a\,e^{-kx_2}\right) e^{-(1-\sqrt{3}/2)\,x_2}\ , \\ \tilde{f}_1(x_2) &= \xi_a\,y_a\,e^{-(1+k-\sqrt{3}/2)\,x_2}\ , \\ f_2(x_1) &= \xi_b\,e^{-x_1} + \xi_{b1}\,e^{-(1+\sqrt{3}/2)x_1}\ , \\ \tilde{f}_2(x_1) &= (2-\sqrt{3})\,\xi_b\,e^{-x_1}\ . \end{aligned} \quad (3.15)$$

The conditions of function matching $f_1(0) = f_2(0)$ and $\tilde{f}_1(0) = \tilde{f}_2(0)$ determine the constants

$$\xi_a = \left(2-\sqrt{3}\right)\xi_b/y_a \quad (3.16)$$

$$\begin{aligned} \xi_{a1} - \xi_{b1} &= \xi_b - \xi_a \equiv \xi_0 \\ &= \sqrt{\frac{\delta_{\text{fit}}}{2g_0}}\,\sqrt{\frac{1}{2-\sqrt{3}}}\left(1 + \frac{2-\sqrt{3}}{2+\sqrt{3}}\,\frac{k-\sqrt{3}}{k}\right). \end{aligned} \quad (3.17)$$

Here, one of the constants, $\xi_{a1} > 0$ or $\xi_{b1} < 0$, can be chosen arbitrarily. At the same time, their difference ξ_0 is uniquely defined and determines the character length within our solution; see also Sec. VI and VII. Below we treat two versions: $\left(\xi_{a1} = 0,\ \xi_0 = |\xi_{b1}|\right)$ and $\left(\xi_0 = \xi_{a1},\ \xi_{b1} = 0\right)$.

The first variant could be sensible for the following reasons. As we take boundary condition (3.8) with $x_2 \gg 1$ [see (3.4)], the distance $\xi^{(1)}$ between the light surface ($r = t$, i.e., $\xi = 0$) and the leading edge of the shell remains nearly constant and equal to ξ_{a1}: Our solution does not describe the variation of this length throughout expansion (from the initial value -1). Really, any shift between the light surface and the leading front could be physically established, in the main, at the earliest stages of expansion $t \gtrsim R_0$, when our treatment does not hold. So within our asymptotical solution for $t \gg R_0$, we could specify the light surface coinciding with the leading boundary and take $\xi_{a1} = 0$. In this case, ξ_0 is associated with the shell thickness h_{shell} in the laboratory system. The value of h_{shell} remains nearly constant during expansion (see Secs. VI and VII) and can be represented therefore within our treatment.

If we accept the second variant with $\xi_{b1} = 0$, the inner boundary conditions approach the self-similar character as directly as possible. But in this case, we must actually expect that ξ_0 determines simultaneously the thickness of the shell, which is constant and can be described by our solution, and the shift $\xi^{(1)}$, which is formed at $t \approx R_0$ and cannot be described by our solution. A particular choice of ξ_{a1} and ξ_{b1} could be done by fitting the exact initial-stage solution ($t \approx R_0$) with our solution for evolved motion. We do not need, however, this operation, beacuse our results are insensitive to this choice: All Lagrangian distributions coincide, while spatial profiles are only shifted with respect to each other.

The solution (3.2), (3.15) gives a complete description of the expanding shell and is characterized by four parameters: ε_{10}, ξ_0, δ_{fit}, and k.

Spatial profiles of hydrodynamic functions at any moment of time t can be found from the equation

$$\xi + \frac{1}{y} - t = 0\ , \quad (3.18)$$

which just expresses the definitions $\xi = t - r$ and $y = 1/r$. As soon as the values ξ and y are specified as functions of x_1 and x_2 by means of (3.2) and (2.18), Eq. (3.18) gives the relation between x_1 and x_2. We can, for example, take a range of values x_1 and obtain the corresponding values of x_2 by solving (3.18). The sets of four variables x_1, x_2, ξ, y completely determine the solution for the ultrarelativistic shell. Using (2.12), we can change variables in the solution from (x_1, x_2) to (τ, φ), so that (2.18), (2.10) give

$$f(\tau, \varphi) = \xi\,e^{\varphi - 2\tau}\ , \qquad \tilde{f}(\tau, \varphi) = \frac{r^2}{2\gamma^2}\,e^{\varphi - 2\tau}\ . \quad (3.19)$$

Finally, using definitions (2.6), (2.9),

$$e^{-2\tau} = r^2\sqrt{\frac{\varepsilon}{\varepsilon_{10}}}\ , \qquad e^{\varphi} = \frac{\gamma}{r}\,\frac{1}{\sqrt{g_0}}, \quad (3.20)$$

we find solutions in the form

$$\gamma = r\sqrt{f/\tilde{f}}\ , \qquad \varepsilon = \varepsilon_{10}\,g_0\,\frac{f\,\tilde{f}}{r^4}\ . \quad (3.21)$$

IV. SELF-SIMILAR SOLUTION FOR RELATIVISTIC SPHERICAL FLOW

In this section, we construct a self-similar solution of relativistic fluid equations with arbitrary γ. Later we shall use this solution to describe the central part of the relativistic fireball. We take the self-similar variable and self-similar functions in the form

$$\eta = \frac{r}{t}, \quad v = V(\eta), \quad \varepsilon = \frac{\mathcal{E}_0}{r^m}\mathcal{E}(\eta), \quad N_b = \frac{\mathcal{N}_{b0}}{r^n}\mathcal{N}_b(\eta). \tag{4.1}$$

Here, $\mathcal{E}_0$ [erg cm^{m-3}], $\mathcal{N}_{b0}$ [cm^{n-3}], m, and n are arbitrary constants. The variable η varies from 0 at the center to $\eta_{\max} \leq 1$ in the outermost layers. In terms of (4.1), fluid equations (1.1), (1.2), (1.4) are reduced to

$$\frac{\eta}{V}\frac{dV}{d\eta} = \frac{1-V^2}{4V}\,\frac{8V - 3m\eta - (8-3m)\eta V^2}{3(V-\eta)^2 - (1-\eta V)^2}, \tag{4.2}$$

$$\frac{\eta}{\gamma^2\mathcal{E}}\frac{d(\gamma^2\mathcal{E})}{d\eta} = \frac{(3m-4)V^2 - \left(\frac{7m}{2}-8\right)\eta V + \left(\frac{3m}{2}-4\right)\eta V^3 - m}{3(V-\eta)^2 - (1-\eta V)^2}, \tag{4.3}$$

$$\frac{\eta}{\gamma\mathcal{N}_b}\frac{d(\gamma\mathcal{N}_b)}{d\eta} = -\frac{(2-n)V + \eta\frac{dV}{d\eta}}{V-\eta}. \tag{4.4}$$

The Lorentz factor is expressed by $\gamma = (1-v^2)^{-1/2} = (1-V^2)^{-1/2}$. The particular case of this solution, with $V \equiv \eta$, $m = 4$, is described in [15]; in this case, Eq. (4.2) becomes an identity and two other equations are reduced to the quadratures. Such a self-similar problem, with equations analogous to (4.2)–(4.4) (with somewhat different notations), is presented also in [19]. However, the author of [19] does not consider expansions at $\eta \to 1$ (see below) and does not indicate and comment on the crucial fact that the total energy and entropy diverge in this limit. Note that the last fact necessarily calls for another, not a similarity, treatment for the outer part of the outflow.

The denominators on the right-hand sides of (4.2)–(4.3) become equal to zero when

$$\left|\frac{V-\eta}{1-\eta V}\right| = \frac{1}{\sqrt{3}}, \tag{4.5}$$

i.e., at the characteristical surface, which moves by a similarity law ($\eta = \text{const}$) with the sound speed relative to the matter.

We look for solutions with zero velocity at the center. The corresponding asymptote at $\eta \to 0$ is

$$V \simeq \frac{m}{4}\eta, \quad \mathcal{E} \simeq \mathcal{E}_c\eta^m, \quad \mathcal{N}_b \simeq \mathcal{N}_c\eta^{m\frac{3-n}{4-m}}, \tag{4.6}$$

where the parameters $\mathcal{E}_c$ and $\mathcal{N}_c$ are defined as follows. Within the expansion (4.6) these parameters are free. Note, however, that the self-similar equations (4.2)–(4.4) are invariant with respect to the scaling of the functions $\mathcal{E}(\eta)$ and $\mathcal{N}_b(\eta)$ by constant factors. It means that different values of $\mathcal{E}_c$ and $\mathcal{N}_c$ only redefine arbitrary coefficients $\mathcal{E}_0$ and $\mathcal{N}_{b0}$ in (4.1); so we accept

$$\mathcal{E}_c = \mathcal{N}_c = 1. \tag{4.7}$$

Assuming that the number of baryons at $r=0$ is a finite nonzero value, we take

$$n = 3m/4. \tag{4.8}$$

Correspondingly, the energy density and baryon concentration at the center decrease with time as

$$\varepsilon(r=0) = \mathcal{E}_0 t^{-m}, \qquad N_b(r=0) = \mathcal{N}_{b0} t^{-3m/4}. \tag{4.9}$$

A self-similar solution for $V(\eta)$ and $\mathcal{E}(\eta)$ is completely determined by only one parameter — the index m (when passing to physical values, we should specify also $\mathcal{E}_0$). $V(\eta)$ for the different m is displayed in Fig. 1. Characteristics (4.5) are shown by dashed lines.

In the outer part of the self-similar solution $\eta \simeq 1$, Eqs. (4.2)–(4.4), have a node with $V \simeq 1$, and all solutions come to this point; see Fig. 1. Introducing

$$\delta = 1-\eta > 0, \qquad \delta_V = 1-V > 0, \tag{4.10}$$

we get an approximate form of Eqs. (4.2), (4.3) near this point ($\delta, \delta_V \ll 1$):

$$\begin{aligned} \frac{dV}{d\eta} = \frac{d\delta_V}{d\delta} &\simeq \frac{4\delta\delta_V - (3m-4)\delta_V^2}{2(\delta^2 - 4\delta\delta_V + \delta_V^2)}, \\ \frac{1}{\gamma^2\mathcal{E}}\frac{d(\gamma^2\mathcal{E})}{d\delta} &\simeq -\frac{(2m-4)\delta - (7m-12)\delta_V}{2(\delta^2 - 4\delta\delta_V + \delta_V^2)}, \end{aligned} \tag{4.11}$$

with $\gamma \simeq 1/\sqrt{2\delta_V}$. There are two corresponding asymptotes. The first is

$$\delta_V \simeq V_1\delta, \qquad \mathcal{E} \simeq \mathcal{E}_1\delta^{-\alpha_1} \qquad (\delta \ll 1), \tag{4.12}$$

where V_1 is the positive root of the square equation $2V_1^2 + 3V_1(m-4) - 2 = 0$ and α_1 is determined by the relation $\alpha_1 = 2[4-m+(2m-4)V_1] / [(3m-4)V_1 - 4]$, while $\mathcal{E}_1$ is arbitrary and can be found, for any m, by

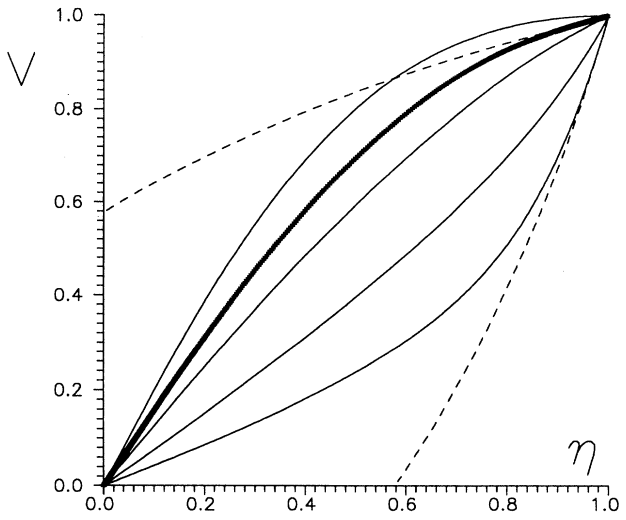

FIG. 1. Self-similar velocity $V(\eta)$ for solutions with different m [see (4.1)] (solid lines); from top to the bottom: $m = 8 > m_{\text{cr1}}$, $m = m_{\text{cr1}} = 4+4/\sqrt{3}$ (bold line), $m = 5$, $m = 3$, and $m = m_{\text{cr2}} = 4-4/\sqrt{3}$. Dashed lines show the characteristics (4.5). Critical solutions $m = m_{\text{cr}\,1,2}$ approach the outermost point ($\eta = 1$, $V = 1$) along the characteristics: with the inclinations $V/\eta = 2 \mp \sqrt{3}$.

numerical integration of the self-similar equations; integration starts from (4.6), (4.7).

We should distinguish two critical solutions with

$$m = m_{\mathrm{cr}\,1,2} = 4 \pm \frac{4}{\sqrt{3}} , \qquad (4.13)$$

which reach the outermost point ($\eta = 1$, $V = 1$) along the characteristic curves (4.5): with the inclinations $V_1 = 2 \mp \sqrt{3}$. As we show below, a critical solution with $m = m_{\mathrm{cr}1} = 4 + 4/\sqrt{3}$ will be of special interest for our problem; in Fig. 1, this case is shown by a bold line. Critical solutions separate different types of self-similar solutions, starting from (4.6), (4.7). As long as $m_{\mathrm{cr}2} \le m \le m_{\mathrm{cr}1}$, integral curves come to the point ($\eta = 1$, $V = 1$) in accordance with (4.12) and describe completely subsonic cases. On the contrary, solutions with $m > m_{\mathrm{cr}1}$ and $m < m_{\mathrm{cr}2}$ cross the characteristics (4.5), which makes these flows supersonic in the outermost part. If $m > m_{\mathrm{cr}1}$, integration typically approaches the second-type asymptote near the leading point:

$$\delta_V \simeq V_2 \delta^2 , \quad \mathcal{E} \simeq \mathcal{E}_2 \delta^{4-m} , \quad \gamma \simeq \frac{1}{\delta \sqrt{2 V_2}} \qquad (4.14)$$

at $\delta \ll 1$, where V_2 and $\mathcal{E}_2$ are free and also can be found numerically.

For the critical solutions, we have $\delta_V \simeq (2 \mp \sqrt{3})\delta$ and $\gamma \simeq 1/\sqrt{2(2 \mp \sqrt{3})\,\delta}$ as $\delta \to 0$. An expansion of the type (4.12) for $\mathcal{E}(\eta)$ should be obtained from (4.2), (4.3) with account of the next-order terms, since the numerator and denominator in the second equation of (4.11) vanish in this case. As a result, we have $\delta_V \simeq (2 \mp \sqrt{3})\delta - (4 \mp 5\sqrt{3}/2)\delta^2$ and

$$\mathcal{E} \simeq \mathcal{E}_{1\mathrm{cr}} \delta^{-\alpha_{\mathrm{cr}}} , \qquad \alpha_{\mathrm{cr}} = \frac{2}{3} \frac{5 \mp 2\sqrt{3}}{2 \mp \sqrt{3}} \qquad (4.15)$$

for $\delta \ll 1$, $m = m_{\mathrm{cr}}$. For the upper sign, we have thus $\alpha_{1\mathrm{cr}} \simeq 3.821$; numerical integration, beginning from (4.6), provides: $\mathcal{E}_{1\mathrm{cr}} \simeq 0.034$. For the lower sign, $\alpha_{2\mathrm{cr}} \simeq 1.512$.

Thus self-similar flow is determined by two quantities: the index m and the dimensional constant $\mathcal{E}_0$ which gives only scaling; see (4.1).

All outer asymptotes show that the total energy within $0 \le \eta \le 1$ diverges for any m, and so a self-similar solution cannot ultimately describe the fireball expansion, but could be joined to another solution for the outermost part of the flow.

V. CENTRAL EXPANSION

In analogy with the nonrelativistic case, we assume that expansion between the center and the leading shell is self-similar. The particular form of the similarity solution [i.e., m and $\mathcal{E}_0$ in (4.1)] should be specified by matching the already given solution with the ultrarelativistic shell—in accordance with our initial assumption that it is the shell motion which determines the central expansion, and not vice versa.

We fit the outer solution for the shell with the inner self-similar solution along the ultrarelativistic characteristic $x_2 = \tau + \varphi/\sqrt{3} = 0$ and at the similarity point $\eta = \eta_{\mathrm{fit}}$; see (3.11). The matching conditions are [see (2.4), (2.6), (2.9), and (4.1)]

$$\gamma = r\sqrt{g_0}\, e^{\varphi} = \gamma(\eta) , \quad \varepsilon = \frac{\varepsilon_{10}}{r^4} e^{-4\tau} = \frac{\mathcal{E}_0}{r^m} \mathcal{E}(\eta) , \qquad (5.1)$$

$$\tau = -\varphi/\sqrt{3} , \qquad \eta = \eta_{\mathrm{fit}} = 1/(1+\delta_{\mathrm{fit}}) . \qquad (5.2)$$

These conditions completely determine the self-similar solution

$$m = 4 + \frac{4}{\sqrt{3}} , \qquad \mathcal{E}_0 = \frac{\varepsilon_{10}}{g_0^{2/\sqrt{3}}} \frac{\gamma^{4/\sqrt{3}}(\eta_{\mathrm{fit}})}{\mathcal{E}(\eta_{\mathrm{fit}})} , \qquad (5.3)$$

where $\mathcal{E}(\eta{=}\eta_{\mathrm{fit}})$ and $\gamma(\eta{=}\eta_{\mathrm{fit}})$ are found by integration of the self-similar equations.

Recalling (4.13), we see that our self-similar solution appears to be the critical one: $m = m_{\mathrm{cr}1}$ (bold line in Fig. 1); i.e., it corresponds to the unit Mach limit and approaches the characteristic curve at $\eta = 1$. This is connected with the choice of the characteristic $\tau = -\varphi/\sqrt{3}$ as the inner boundary for the relativistic shell. We may expect that a critical self-similar solution with $m = m_{\mathrm{cr}2} = 4 - 4/\sqrt{3}$ would be fitted with the shell solution if the characteristic $\tau = \varphi/\sqrt{3}$ was chosen as the inner boundary of the shell, but such a solution is not self-supported, because the energy density in the shell would drop faster than at the center, leading to a dissolving of the shell [see (5.6)].

As we consider $\eta_{\mathrm{fit}} \simeq 1$ for the narrow ultrarelativistic shell, we can employ the expansion (4.15) for $\delta_{\mathrm{fit}} \ll 1$ in (5.1) and thus express analytically the constant $\mathcal{E}_0$:

$$\mathcal{E}_0 \simeq \frac{1}{\mathcal{E}_{1\mathrm{cr}}} \left[4 - 2\sqrt{3}\right]^{-\frac{2}{\sqrt{3}}} \varepsilon_{10}\, g_0^{-\frac{2}{\sqrt{3}}}\, \delta_{\mathrm{fit}}^{\alpha_{\mathrm{cr}} - \frac{2}{\sqrt{3}}} . \qquad (5.4)$$

Let us consider the matching point in more detail. Using (5.1) with an arbitrary η, one can find the curve $\tau(\varphi)$ within the self-similar solution. For the outermost part of the self-similar solution, expansion (4.15) reduces this curve to $\tau \propto -\alpha_{\mathrm{cr}}\varphi$, whose inclination does not coincide with $\tau = -\varphi/\sqrt{3}$ at the inner characteristic of the ultrarelativistic shell. Thus we have a weak discontinuity at the matching point. Note, however, that if our self-similar solution could overcome sound velocity and approach the second-type asymptote (4.14), there would be

$$\varepsilon \propto e^{-4\tau} \propto \mathcal{E} \propto \delta^{4-m} \propto \gamma^{m-4} \propto e^{(m-4)\varphi} = e^{4\varphi/\sqrt{3}} \qquad (5.5)$$

for $m = m_{\mathrm{cr}1} = 4 + 4/\sqrt{3}$, which just gives the relation $\tau = -\varphi/\sqrt{3}$. Thus our self-similar solution also reproduces this regime; the interval of transition to this law is degenerated into a point.

In accordance with (4.9), the energy density and baryon concentration at the center drop with time ac-

cording to the laws

$$\varepsilon(r=0) = \frac{\mathcal{E}_0}{t^{4+4/\sqrt{3}}} \ , \quad N_b(r=0) = \frac{\mathcal{N}_{b0}}{t^{3+3/\sqrt{3}}} \ , \qquad (5.6)$$

which is faster than inside the shell ($\varepsilon \propto t^{-4}$, $N_b \propto t^{-3}$). This is because the center is related to the minimum of the energy distribution, and expansion of the central caverne additionally decreases ε and N_b as the shell moves outwards. The total energy within self-similar flow ($0 \le \eta \le \eta_{\rm fit}$) diminishes with time as t^{3-m}.

VI. BASIC PARAMETERS OF THE SOLUTION AND NUMERICAL RESULTS

Our solution for the relativistic fireball is determined by the quantites ξ_0, ε_{10}, $\delta_{\rm fit}$, and k. Let us consider how these values are related to the input parameters of the problem: the released energy E_0 and the initial radius R_0.

The quantity ξ_0 [see (3.17)] determines the character length of the problem and is associated with the shell thickness $h_{\rm shell}$ in the laboratory frame. As follows from our calculations, this thickness remains nearly constant during expansion: The maximum of energy density is reached at $\xi \simeq \xi_0$, while $\sim 80\%$ of the fireball entropy is concentrated in the outer layer $0 \le \xi \le 2\xi_0$. Thus we define

$$h_{\rm shell} = 2\xi_0 = \sqrt{\frac{\delta_{\rm fit}}{g_0}\frac{2}{2-\sqrt{3}}}\left(1+\frac{2-\sqrt{3}}{2+\sqrt{3}}\frac{k-\sqrt{3}}{k}\right). \qquad (6.1)$$

As $k > \sqrt{3}$, the second term in parentheses is smaller than the first term, and so $h_{\rm shell}$ nearly does not depend on k and can be given by

$$h_{\rm shell} \simeq \sqrt{\frac{\delta_{\rm fit}}{g_0}}\sqrt{\frac{2}{2-\sqrt{3}}} \simeq 3\sqrt{\frac{\delta_{\rm fit}}{g_0}} \ . \qquad (6.2)$$

Numerical calculations [1] have shown that the thickness of the ultrarelativistic shell is approximately equal to the initial radius R_0 of the fireball. It seems clear that within our treatment these lengths $h_{\rm shell}$ and R_0 are also originally connected with each other and with the shift ξ_0. Really, the outflow cannot be ultimately described by a self-similar solution since there exists the initial radius of the problem. Respectively, the self-similar part of our solution breaks in the outer layer of the corresponding thickness and should be matched with the shell solution. Within the matching procedure, we actually need the shifting length ξ_0 in order to fit the light surfaces ($r = t$) of the shell solution and of the self-similar solution, because the last does not know about both lengths. So we also can assume that $h_{\rm shell}$ is roughly equal to the initial radius: $h_{\rm shell} \simeq R_0$.

Note that the result $h_{\rm shell} = {\rm const}$ is not an artifact of our construction. On the contrary, the shell solution is applied to the outer region $\xi < \delta_{\rm fit}\, t \propto t$, widening with time.

The product ($\varepsilon_{10} g_0$) specifies the scale of energy and is determined by total energy of explosion E_0. At the same time, ε_{10} alone does not influence the form of all physical distributions since original fluid equations (1.1)–(1.3) are linear with respect to ε (or $\varepsilon^{3/4}$). The total energy is expressed as

$$E_0 = 4\pi\int_0^t \gamma^2 \varepsilon r^2 dr \simeq 4\pi g_0 \varepsilon_{10}\int_0^{\text{few } h_{\rm shell}} e^{2\varphi-4\tau} d\xi \ . \qquad (6.3)$$

Within all solutions, the integral over ξ is almost universally proportional to $h_{\rm shell}$ with the factor 1.2–1.4. The comoving entropy s per unit volume is $s = s_0\, e^{-3\tau}/r^3$ ($s + 0 = {\rm const}$), so that the entropy $S(r)$ inside a layer with radius r can be written as

$$S(r) \ = \ 4\pi \int_0^r \gamma\, s\, r^2\, dr \ = \ 4\pi\, s_0\, \sqrt{g_0} \int_0^r e^{\varphi-3\tau}\, dr \, ; \qquad (6.4)$$

below we use S as a Lagrangian coordinate. The total entropy of the fireball is $S_0 = S(r=t)$, and the last integral, in the limit $r = 0$–t, is also proportional to $h_{\rm shell}$ with nearly the same factor 0.21–0.23. For a convenient presentation of numerical results in the figures, we take $h_{\rm shell} = 1$; i.e., treat r, t, ξ in units of the shell thickness.

The particular value of $\delta_{\rm fit} \ll 1$ (at fixed $h_{\rm shell}$) plays no principle role in physical distributions, but it is connected with the scale of Lorentz factors. Really, for any moment of time, we can specify the average bulk Lorentz factor of the fireball as the value $\gamma(\xi) \equiv \gamma_0$ related to the maximium of the laboratory frame entropy $s_{\rm lab}(\xi)$, since most of the expanding material is concentrated here. The corresponding quantities $\varphi_0 \equiv \varphi|_{s_{\rm lab}={\rm max}}$ and $\tau_0 \equiv \tau|_{s_{\rm lab}={\rm max}}$ are nearly constant at late time for each solution; see (7.5), (7.7). So the average Lorentz factor can be given by

$$\gamma_0 \ \equiv \ \gamma|_{s_{\rm lab}={\rm max}} \ = \ \sqrt{g_0} e^{\varphi_0} t \ . \qquad (6.5)$$

The parameter g_0 can be expressed from (6.1) leading to $\gamma_0 \simeq 3\,\delta_{\rm fit}\, e^{\varphi_0} t/h_{\rm shell}$. Thus $\delta_{\rm fit}$ determines the coefficient within linear growth of γ_0 with time [and within linear widening of the shell's comoving thickness $h_{\rm com} \simeq h_{\rm shell}\gamma_0 \propto t$, if we roughly define the comoving frame as moving with the Lorentz factor (6.5)].

The character scale of γ is evidently associated with the original ratio E_0/M_0 of the released energy to the fireball rest mass. Within the ultrarelativistic equation of state accepted so far, we actually consider the limit $E_0/M_0 \to \infty$, and this ratio falls out from our treatment, leaving γ scale free. The value of $\delta_{\rm fit}$ could be chosen, therefore, for the reasons of optimal fitting of our solution with the solutions for the following stage of free expansion, where the average γ saturates at E_0/M_0 [1].

Power index k is connected with the particular initial conditions — primarily, with the structure of the initial rarefaction wave. If we assume that this structure does not differ significantly from the plane-parallel one (corre-

sponding to $k=\sqrt{3}$), then k would only slightly exceed $\sqrt{3}$. Note also that, as $k \to \sqrt{3}$, the dependence of ξ_0 (6.1) and of all profiles upon k nearly vanishes, which makes this limit most universal.

We could add that, as follows from (5.4), (6.1), and (6.3), the dimensional constant $\mathcal{E}_0$ of the the self-similar solution is rather insensitive both to k and $\delta_{\rm fit}$. This agrees with the basic idea of the self-similar solution, that the self-similar flow forgets about the particular initial conditions.

As a specific example, we consider the case

$$\delta_{\rm fit} = 10^{-2} , \qquad k = 1 + \sqrt{3}/2 ; \tag{6.6}$$

fitting with the self-similar solution is carried at $\gamma \simeq$ 13. The main results of the calculations are presented in Figs. 2–5. In Figs. 2 and 3 we show the distributions of entropy density s and $s_{\rm lab}$ and of the Lorentz factor γ over the Lagrangian coordinate $S(r)$ at consequent moments of time.

Comparison with numerical results [1] shows good qualititative and satisfactory quantitative coincidence. Laboratory-frame distributions look not so flat as in [1], but in Sec. VIII, we modify our solution to get better agreement and to account for different initial energy distributions. Spatial profiles $s(\xi)$ and $s_{\rm lab}(\xi)$ for the moment $t = 10^4$ are displayed by solid lines in Fig. 4 [with $\xi_{a1}=0$ in (3.15)] and are similar to the numerical results of [2]. Figure 5 shows the corresponding dependences $x_2(x_1)$ (solid lines).

Spatial distributions in the laboratory frame strongly depend on the choice of $h_{\rm shell}$. We are interested, however, mainly in the comoving-frame values, in terms of which all physical processes inside the fireball can be described most easily.

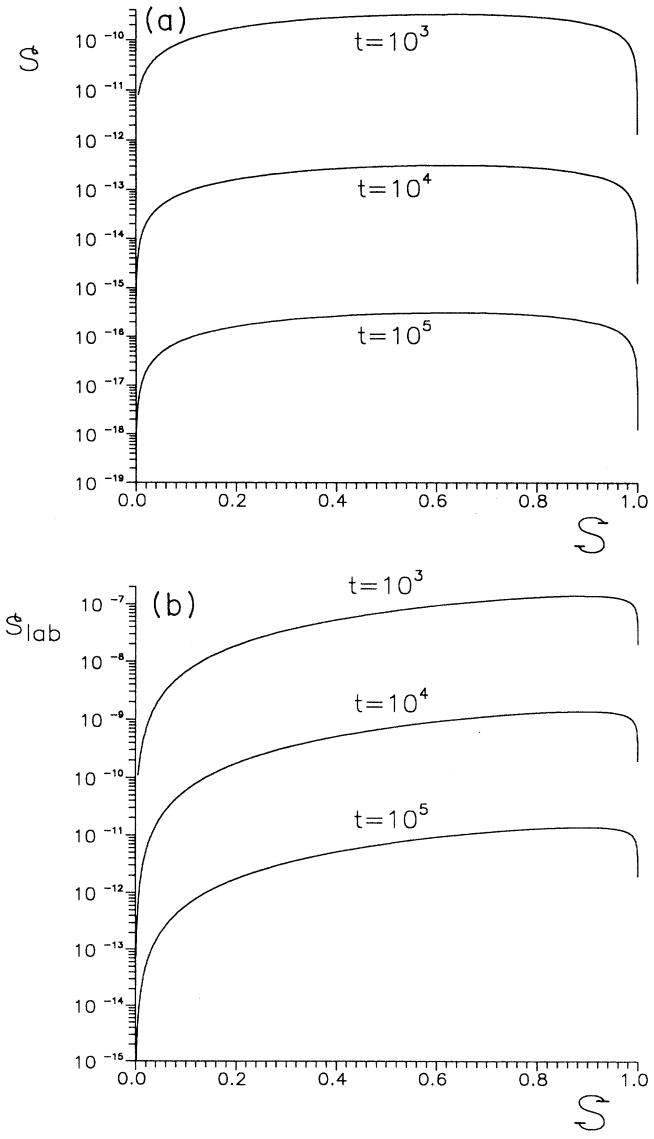

FIG. 2. (a) Distribution of the comoving-frame entropy density s over the Lagrangian coordinate S at consequent moments of time; see Sec. VI. (b) Laboratory-frame entropy density $s_{\rm lab}$ over the Lagrangian coordinate.

VII. APPROXIMATE RELATIONS AND THE LIMITING SOLUTION AT $t \gg h_{\rm shell}$

Here, we present the aproximate forms of our solution which significantly simplify the treatment, giving results very close to exact ones.

First, we can use approximate relations for Bessel functions I_0 in (3.2). Our exact results show that the arguments of Bessel functions never exceed 1: At fixed t, the curve $x_2(x_1)$ is always close to the boundary axes $x_1=0$ and $x_2=0$; see Fig. 5. Hence, we can use the expansion $I_0(z) \simeq 1+z^2/4$ at small z:

$$I_0\left(\sqrt{x_1\,(x_2-x_2')}\right) \simeq 1 + \frac{x_1\,(x_2-x_2')}{4} ,$$
$$I_0\left(\sqrt{(x_1-x_1')\,x_2}\right) \simeq 1 + \frac{(x_1-x_1')\,x_2}{4} , \tag{7.1}$$

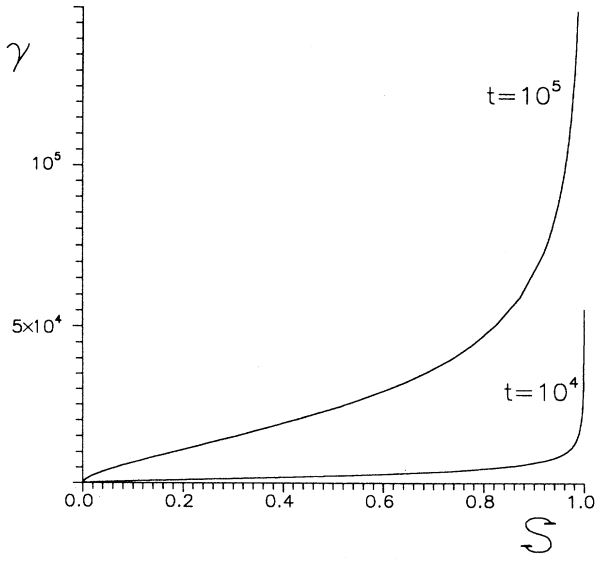

FIG. 3. The bulk Lorentz factor γ over the Lagrangian coordinate.

which gives

$$f(x_1,x_2) \approx f_1(x_2) + f_2(x_1) - f_1(0)\left(1+\frac{x_1x_2}{4}\right) + \frac{x_1}{4}\int_0^{x_2} f_1(x_2')\,dx_2' + \frac{x_2}{4}\int_0^{x_1} f_2(x_1')\,dx_1' \tag{7.2}$$

and the same relation for $\tilde{f}$ with $\tilde{f}_1(x_2)$ and $\tilde{f}_2(x_1)$. Introducing here the specific boundary functions (3.15), one can take the definite integrals and present a solution in algebraic form. Our calculations confirm that the profiles obtained by using (7.3) and those with exact expressions for I_0 absolutely coincide in the graphics. Moreover, if we take $I_0=1$ throughout solution, so that

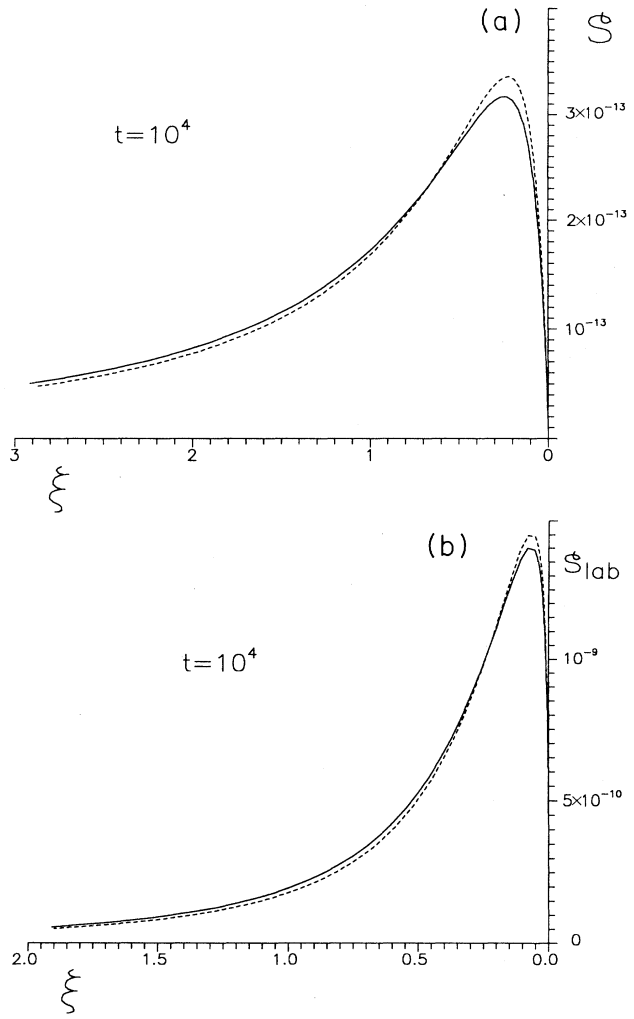

FIG. 4. (a) Spatial profile of the comoving-frame entropy density at the moment $t = 10^4$ (solid line). Dashed curve presents the case $I_0 = 1$ [see (7.3)] and coincides with the approximate analytical solution (7.6) (b) Spatial profile $s_{\rm lab}(\xi)$ at $t = 10^4$ within ultrarelativistic shell (solid line). The dashed curve presents the case $I_0 = 1$ [see (7.3)] and coincides with the approximate analytical solution (7.6).

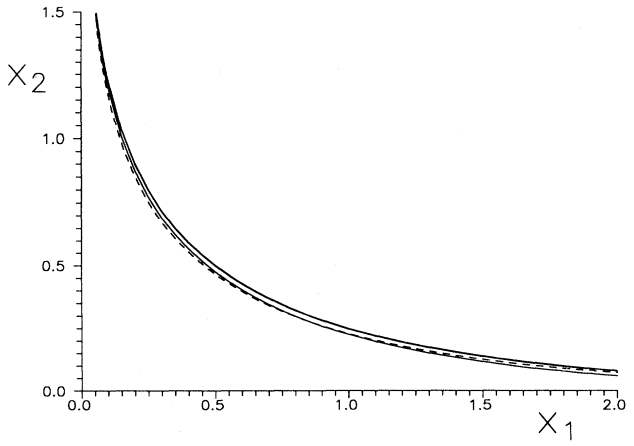

FIG. 5. Dependences $x_2(x_1)$ [these parameters are defined in (2.12)] within the shell solution for the same moments of time as in Figs. 2 and 3 (solid lines). The dashed curve shows approximate solution (7.6).

$$\begin{aligned} f &\approx f_1(x_2) + f_2(x_1) - f_1(0)\ , \\ \tilde{f} &\approx \tilde{f}_1(x_2) + \tilde{f}_2(x_1) - \tilde{f}_1(0)\ , \end{aligned} \tag{7.3}$$

this produces the difference in spatial profiles not more than a few percent in comparision with exact I_0 (see Fig. 4, where approximate curves are given by the dashed lines); corresponding distributions over Lagrangian mass coordinates (Figs. 2,3) are undistinguished.

Second, Eq. (3.18), giving the relations between all physical values for ultrarelativistic shell at any moment t, is worth reducing to

$$\frac{\xi(x_1,\,x_2)}{t} + 1 - ty(x_1,\,x_2) = 0 \tag{7.4}$$

when we account for the fact that $\xi \ll t$ at late times for most part of the shell, i.e., that the shell is narrow. Really, our profiles obtained by solving (3.18) and (7.4) are undistinguished at $t/R_0 > 10/\delta_{\rm fit}$. Equation (7.4) places the functions ξ and y in different terms and only in numerators, which is convenient for calculations and especially for analytical estimates. In particular, (7.4) gives $dy = d\xi\,/\,t^2$ $(t=\text{const})$, to be employed when we determine the points of maximal temperature, entropy, and energy density inside the shell:

$$\left.\frac{d\tau}{d\xi}\right|_{\substack{T,s,\varepsilon\\=\max}} = \left.\frac{3d\tau - d\varphi}{2\,d\xi}\right|_{\substack{s_{\rm lab}\\=\max}} = \left.\frac{2d\tau - d\varphi}{d\xi}\right|_{\substack{\varepsilon_{\rm lab}\\=\max}} = \frac{1}{t} \tag{7.5}$$

at $t = \text{const}$; the maximum of $T_{\rm lab}$ is specified by the relation $d\tau = d\varphi$. Maximums of all the comoving–frame values are defined by one relation, since these values are connected by exact power laws $\varepsilon \propto s^{4/3} \propto T^4$.

Thus for any fixed moment of time, spatial profiles within ultrarelativistic shell can be described by Eq. (7.4) where all terms are expressed via algebraic relations (2.18), (3.15), (7.2) [or even (7.3)].

And finally we derive a very simple approximate asymptotical form of our solution at $t \gg h_{\rm shell} \simeq R_0$. In this limit, we have $r \approx t$ for most layers of the shell; i.e., Eq. (3.18) [or (7.4)] is reduced to $y \approx 1/t \to 0$ (note that we take r and t in units of $h_{\rm shell}$). This implies $\tilde{f} \approx 0$. Taking for simplicity $I_0 = 1$ and expressing $\tilde{f}$ from (7.3), (3.15), we see that the functions x_1 and x_2 are asymptotically connected as

$$e^{-(1+k-\sqrt{3}/2)\,x_2} = 1 - e^{-x_1} \quad . \tag{7.6}$$

In Fig. 5, curve (7.6) is given by a dashed line, and one can see that exact curves are really very close to this limiting behavior at late times. Spatial profiles obtained with (7.6) coincide with the dashed curves in Fig. 4 [as we take $I_0 = 1$ in $\tilde{f} = 0$ for getting (7.6)], while corresponding distributions over Lagrangian coordinates (Figs. 2, 3) coincide with exact ones.

Using (7.6) and taking $1/t \approx 0$ in (7.5) we can find analytically the maximum points of the hydrodynamic functions. In practice, the point of interest is the maximum of $s_{\rm lab}$. It is related to the main part of the expanding gas, and so the corresponding value $\varphi = \varphi_0$ determines actually the average bulk Lorentz factor of the fireball [see (6.5)], whereas $\tau = \tau_0$ determines the character temperature. After transformations, we obtain

$$\begin{aligned} \varphi_0 &= \frac{\sqrt{3}}{2}\left(\frac{\ln\left[c_m/(c_m-1)\right]}{1+k-\sqrt{3}/2} - \ln c_m\right) \quad , \\ \tau_0 &= \frac{\ln\left[c_m/(c_m-1)\right]}{2\,(1+k-\sqrt{3}/2)} + \frac{\ln c_m}{2} \quad , \end{aligned} \tag{7.7}$$

where

$$c_m = 1 + \frac{\sqrt{3}-1}{\sqrt{3}+1}\,\frac{1}{1+k-\sqrt{3}/2} \quad . \tag{7.8}$$

For our numerical example $k = 1 + \sqrt{3}/2$, this gives $\varphi_0 = 0.816$, $\tau_0 = 0.597$ (calculations with exact I_0 give 0.77 and 0.594).

VIII. FAMILY OF FIREBALL SOLUTIONS

We can easily modify the above treatment to get a whole family of fireball solutions, where different solutions are related to different regimes of initial energy deposition. We redefine the inner boundary conditions for the ultrarelativistic shell in a more general form than (3.14) and take

$$\xi^{(2)} = \xi_{b1} + \xi_b e^{-\beta\, x_1} \quad , \tag{8.1}$$

introducing a new free parameter β. Our previous solution (Sec. III) with $\xi^{(2)} \propto t$ corresponds to $\beta = -\sqrt{3}/2$, and this is the minimal possible value of β, because the inner boundary of the shell should not approach the center; so $\xi^{(2)}$ should not grow faster than linearly with time. Positive β would mean that we originally assume constant laboratory-frame thickness of the shell $h_{\rm shell} \simeq \xi_{b1}$. Equations (2.20), (8.1) lead to

$$y_1^{(2)} = y_b\,\xi_b\, e^{-\beta\, x_1} \quad , \qquad y_b = -\beta\,\frac{2-\sqrt{3}}{\beta+\sqrt{3}} \tag{8.2}$$

instead of (3.13). Thus the two last relations of (3.15) would be replaced by

$$\begin{aligned} f_2(x_1) &= \xi_{b1}\, e^{-(1+\sqrt{3}/2)x_1} + \xi_b\, e^{-(\beta+1+\sqrt{3}/2)x_1} \quad , \\ \tilde{f}_2(x_1) &= y_b\,\xi_b\, e^{-(\beta+1+\sqrt{3}/2)x_1} \quad . \end{aligned} \tag{8.3}$$

For the leading boundary, we again use Eqs. (3.8), (3.9) and, correspondingly, the first two relations of (3.15); y_a is given in (3.9), and we take $\xi_{a1} = 0$ for the reasons discussed in Sec. III. Matching of boundary functions at $x_1 = x_2 = 0$ specifies the parameters

$$\xi_a = \frac{y_b\,\xi_b}{y_a} \quad , \qquad \xi_b = \frac{\xi_{b1}}{1 + y_b/y_a} \quad . \tag{8.4}$$

The boundary problem (3.1) is determined therefore by the length ξ_{b1}, which is evidently of order of $h_{\rm shell}$ (for $\beta > 0$, $\xi_{b1} \simeq h_{\rm shell}$) and two power indices $k > \sqrt{3}$ and $\beta \geq -\sqrt{3}/2$. Both indices could be associated with the initial energy distribution: k mostly with the rarefaction wave, whereas β could be related primarily to the central structure and describe different physical situations. In practice, the values $\beta = 3$–5 give the best agreement with numerical results of [1]. In this work, initial distribution of energy is taken steplike, and Lagrangian distributions within evolved expansion are also flat. Large $\beta > 5$ seem to correspond to the case where the initial energy is maximal at the center, and these solutions could reproduce the results of [2]. On the contrary, our previous solution with minimal $\beta = -\sqrt{3}/2$ is likely to represent the limiting situation, where primarily the outermost envelope of the initial object is accelerated, forming a fireball; this variant could be especially relevant to GRB models.

In Fig. 6, we display the distribution of the laboratory-frame entopy over the Lagrangian coordinate inside the shell [analogue of Fig. 2(b)] for $\beta = 5$, $k = 1 + \sqrt{3}/2$.

The dimensional solution is specified also by the parameters ε_{10} and g_0 from (2.6) and (2.9). The product $(\varepsilon_{10}\, g_0)$ gives the scale of energy related to the explosion energy E_0, just similarly to our previous solution. The constant g_0 (with r, t taken in units of $h_{\rm shell}$) is associated with the scale of the outflow Lorentz factor; see Eq. (6.5), which also holds here, and the following discussion. Thus g_0 could be detemined by matching with the following free-expansion solutions.

The approximate asymptotical form of new solutions at $t \gg h_{\rm shell} \simeq R_0$, similar to (7.6), reads

$$e^{-(1+k-\sqrt{3}/2)\,x_2} = 1 - e^{-(\beta+1+\sqrt{3}/2)\,x_1} \quad . \tag{8.5}$$

The maximum of $s_{\rm lab}$ can be approximately calculated by using (7.7) with more general c_m instead of (7.8):

$$c_m = 1 + \frac{\sqrt{3}-1}{\sqrt{3}+1}\,\frac{1+\beta+\sqrt{3}/2}{1+k-\sqrt{3}/2} \quad . \tag{8.6}$$

We again assume that the central part of the fireball

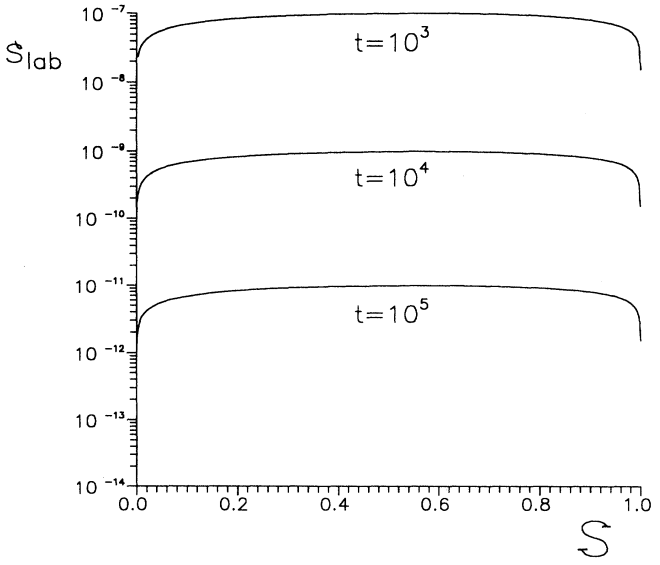

FIG. 6. Laboratory frame entropy density $s_{\rm lab}$ over the Lagrangian coordinate within the shell-solution of Sec. VIII with $\beta = 5$, $k = 1 + \sqrt{3}/2$.

expands in a self-similar manner. Below we consider only the case $\beta > 0$ with $\xi^{(2)} \simeq \text{const} = \xi_{b1}$. The self-similar coordinate $\eta_{\rm fit}$, where we join a similarity solution to the shell solution, now quickly tends to 1 with time:

$$\eta_{\rm fit} = \frac{r}{t} = \frac{t - \xi_{b1}}{t} = 1 - \frac{\xi_{b1}}{t} , \qquad (8.7)$$

so that $\delta_{\rm fit} = 1 - \eta_{\rm fit} = \xi_{b1}/t$ is automatically small at late t. The matching procedure demands that the energy density and Lorentz factor in this point vary with time, following the shell solution [see (2.4)]:

$$\gamma \propto t , \qquad \varepsilon \propto t^{-4} . \qquad (8.8)$$

Introducing possible self-similar asymptotes at $1-\eta = \delta = \delta_{\rm fit} \ll 1$, we see that any supersonic expansion (4.14) satisfies these conditions, and direct fitting implies

$$\varepsilon_{10}\, g_0^{-2/\sqrt{3}}\, \xi_{b1}^{m-(4+4/\sqrt{3})} = \mathcal{E}_0\, \mathcal{E}_2\, (2\, V_2)^{2/\sqrt{3}} , \qquad (8.9)$$

where the shell-solution parameters are placed on the left-hand side, while parameters of the self-similar solution on in the right. If we assume that the last ones should not explicitly depend on the shifting length ξ_{b1}, we again obtain

$$m = 4 + \frac{4}{\sqrt{3}} = m_{\rm cr1} . \qquad (8.10)$$

IX. CONCLUSIONS

We have derived an analytical solution describing spherical expansion of a highly relativistic fireball into the vacuum. This solution presents an intermediate asymptote within the whole process of the fireball outflow. On the one hand, we consider evolved expansion with $t \gg R_0$ (where R_0 is the initial radius), which allows us to separate the shell solution and self-similar solution. On the other hand, our treatment is related to the early stages of expansion when the fireball is hot and dense: We use an ultrarelativistic equation of state, assume that the flow is adiabatic (optically thick), and neglect the ambient material and corresponding shocks.

Our solution can be presented mathematically in a very simple approximate form [see (7.6), (8.5)] and thus allows us to make any physical estimates for this stage of expansion as well as to treat the resulting analytical distributions as the initial conditions for the following motion. It seems also very possible that a similar treatment with an approximate account of the particle rest masses could provide a self-consistent fitting with the next-stage solutions, because the final free expansion can be again described analytically.

We have constructed this solution primarily in the context of the GRB models, but it may be also applied to the hydrodynamic stage of particle outflow, resulting from electron-positron annihilation into hadrons. Within the last process, original particles disappear and the system loses information about initial nonsymmetry, which makes the following expansion of the secondary particles spherically symmetric and initial distributions for the secondary flow uncertain; our boundary-problem treatment (avoiding initial conditions) could be especially applicable to this case.

We may also assume that our solution could be extended to the cases of nonspherical expansion (typical for colliders, for cosmic ray interaction with the atmospherical particles, etc.) — to the stages when the outflow acquires conical character. For example, as shown in [7], relativistic outflow starting from $\sim$ plane geometry, evolves to conical expansion, with the angle distributions established in the transition phase. If tangential heat fluxes become smaller than radial ones, angle distributions are more or less fixed (and not spherical), while radial profiles could be roughly described by spherical-type solutions with different total energies in different directions. However, this question calls for special consideration.

G.S.B.-K. acknowledges support from the Russian Fundamental Research Foundation (93-02-17106), the Russian Ministry of Science (3-169), and the International Science Foundation (M 34000). The work of M.V.A.M. was supported, in part, by the Russian Fundamental Research Foundation (93-02-17114), by the International Science Foundation (M9E000), and by the Tomalla Foundation (in the framework of the research program of the International Center for Fundamental Physics in Moscow). Both authors appreciate support from the Scientific and Educational Center of Kosmomicrophysics "KOSMION."

[1] P. Meszaros, P. Laguna, and M. J. Rees, Astrophys. J. **415**, 181 (1993).
[2] T. Piran, A. Shemi, and R. Narayan, Mon. Not. R. Astron. Soc. **263**, 861 (1993).
[3] O. F. Prilutski and V. V. Usov, Astrophys. Space Sci. **34**, 395 (1975).
[4] B. Paczynski, Astrophys. J. Lett. **308**, L43 (1986).
[5] A. H. Taub, Phys. Rev. **74**, 328 (1948).
[6] L. D. Landau and E. M. Lifshitz, *Fluid Mechanics* (Pergamon, London, 1959).
[7] L. D. Landau, Ann. Sov. Acad. Sci. Phys. **17**, 51 (1953); see also L. D. Landau, *Collected Papers* (Nauka, Moscow, 1959), pp. 153, 260.
[8] I. M. Khalatnikov, Sov. Phys. JETP **27**, 529 (1954).
[9] A. V. Byalko, JETP Lett. **29**, 196 (1979).
[10] P. Meszaros and M. J. Rees, Mon. Not. R. Astron. Soc. **257**, 29P (1992).
[11] P. Meszaros and M. J. Rees, Astrophys. J. **405**, 278 (1993).
[12] M. Begelman, P. Meszaros, and M. J. Rees, Mon. Not. R. Astron. Soc. **265**, L13 (1993).
[13] Ya. B. Zel'dovich and Yu. P. Raizer, *Physics of Shock Waves and High Temperature Hydrodynamic Phenomena* (Academic, New York, 1966).
[14] F. Cooper, G. Frye, and E. Schonberg, Phys. Rev. D **11**, 192 (1975).
[15] Yu. P. Ochelkov, O. F. Prilutski, I. L. Rozental, and V. V. Usov, *Relativistic Kinetics and Hydrodynamics* (Atomizdat, Moscow, 1979).
[16] G. C. Pomraning, *The Equations of Radiational Hydrodynamics* (Pergamon, Oxford, 1973).
[17] R. Courant, *Partial Differential Equations* (Interscience, New York, 1962).
[18] V. I. Smirnov, *Kurs Vys'shej Matematiki* (Nauka, Moscow, 1967), Vol. 2, Sec. 185.
[19] N. R. Sibgatullin, *Oscillations and Waves in Strong Electromagnetic and Gravitational Fields* (Nauka, Moscow, 1984).